https://doi.org/10.70882/48shyr84

SCIENCE FORUM (JOURNAL OF PURE AND APPLIED SCIENCES) 26, (5 Special) (2026), 256 - 280

Science Forum (Journal of Pure and Applied Sciences)

Journal Homepage: https://atbuscienceforum.com.ng/index.php/jpas

Quantitative Assessment of Hypermucoviscosity and Siderophore Production in Clinical Isolates of Hypervirulent *Klebsiella pneumoniae* under Iron-Restriction Stress: Virulence Genotype, Capsular Serotype, Carbapenemase Carriage and Clinical Outcome in Al-Anbar, Iraq.

Intisar Hameed Ali Al-Abdali
Ministry of Education, General Directorate of Education in Anbar

Abstract

Hypervirulent *Klebsiella pneumoniae* (hvKp) is still identified at the bench by the string test, a binary reading of a continuous phenotype. Whether quantitative measures of mucoviscosity and iron acquisition define the pathotype more faithfully than that single threshold has not been settled in Middle Eastern settings, where carbapenem resistance is endemic. Two hundred and forty consecutive clinical *K. pneumoniae* isolates recovered at a tertiary referral centre in Al-Anbar, Iraq, were cultured under iron-restricted and iron-saturated conditions. Hypermucoviscosity was quantified as string-test length and capsular uronic acid concentration; siderophore output was measured by the chrome azurol S assay in µg/mL and percentage siderophore units. Relative expression of *iucA* and *iroB* was determined by 2^−ΔΔCt after reference-gene stability testing. Five virulence markers, capsular serotype and *bla*NDM, *bla*OXA-48 and *bla*OXA-51 were detected by PCR. Death was modelled by binary logistic regression. All four quantitative measures were mutually correlated (Spearman ρ = 0.783, 0.566, 0.528, 0.505, 0.444 and 0.357; all $P < 0.001$) and differed significantly by capsular type (all Kruskal–Wallis $P < 0.001$). Siderophore output followed a threshold rather than a dose–linear pattern: median CAS concentrations were 15.03, 14.54 and 16.91 µg/mL at 0, 1 and 2 virulence markers, rising to 52.64, 47.65 and 44.73 µg/mL at 3, 4 and 5 markers. A marker count ≥3 predicted the published CAS cut-off of 30 µg/mL with AUC 0.964 (sensitivity 94.5%, specificity 97.8%). CAS concentration discriminated genotypic hypervirulence better than the string test (AUC 0.989 vs 0.926; ΔAUC 0.063, 95% CI 0.027–0.106; $P < 0.001$), the loss residing in string-test specificity (62.5% vs 98.4%) rather than sensitivity (91.1% vs 92.9%; κ = 0.383). Iron restriction induced *iucA* 4.62-fold (IQR 3.84–5.31) and *iroB* 5.23-fold (IQR 4.24–5.93); both $P < 0.001$, with a stable *rpoB* ($P = 0.665$). In the adjusted model, only virulence-marker burden independently predicted death (OR 1.39 per additional marker, 95% CI 1.02–1.88; $P = 0.036$; model AUC 0.755). In this population the hypervirulent phenotype is internally coherent and threshold-defined. A genotype of ≥3 markers coupled with quantitative CAS measurement at ≥30 µg/mL outperforms the conventional string test, and should anchor the operational definition of hvKp in comparable settings.

Keywords
Hypervirulent *Klebsiella Pneumoniae;*
Siderophore;
Hypermucoviscosity;
String Test;
Iron Restriction;
iucA; iroB;
Carbapenem Resistance.

EISSN: 3156-5190 (Online)
ISSN: 1119-4618 (Print)
JPAS
Faculty of Science, ATBU Bauchi

Corresponding Author: Intisar Hameed Ali Al-Abdali, Ministry of Education, General Directorate of Education in Anbar Email: amsayf77@gmail.com
© 2026 Faculty of Science, ATBU Bauchi. All rights reserved

1. Introduction

The separation of classical *Klebsiella pneumoniae* (cKp) from its hypervirulent variant began as a bedside observation and hardened, perhaps too quickly, into a laboratory rule (Chang *et al.,* 2021). Isolates recovered from pyogenic liver abscess, endophthalmitis and metastatic infection formed mucoid colonies that stretched on loop withdrawal, and the five-millimetre threshold that followed has served clinical laboratories for two decades without ever acquiring the status of a reference standard (AL-FAHDAWI *et al.,* 2023; Lan et al., 2021). That gap has widened as the two pathotypes have converged (Arcari & Carattoli, 2022).

Convergence is the defining epidemiological fact of the past decade. Hospital-adapted multidrug-resistant clones have acquired hvKp-defining virulence plasmids, while hypervirulent clones have acquired carbapenemases, yielding strains that carry the traits of both lineages simultaneously (Abbas *et al.,* 2024; Liao *et al.,* 2024). Experimental work has shown how directly this can occur: hybrid pLVPK-like conjugative plasmids carrying both virulence and carbapenem-resistance determinants readily convert an ST11 carbapenem-resistant strain into a carbapenem-resistant hypervirulent one (Han *et al.,* 2022). The resulting strains have been reported across Asia, Europe and the Americas, with ST11, ST23 and ST258 as the principal vehicles (Xie *et al.,* 2021). Whether they are proportionally more lethal than classical carbapenem-resistant strains is disputed. Studies report conflicting mortality estimates depending on the method used to define hypervirulence. This suggests that these discrepancies cannot be dismissed, and it is the reason this study treats measurement as a substantive question rather than a technical detail.

Three biological features structure the phenotype. The first is the capsule. Capsular polysaccharide, built largely from uronic acid residues, resists phagocytosis and complement deposition, and its production is regulated by *rmpA*, *rmpA2*, *rmpC* and *rcsB* (Zhu *et al.,* 2021). Regulator and phenotype are not, however, the same thing. Mutants with reduced capsule expression can retain hypermucoviscosity, and promoter polymorphism in *rmpA* — strong P11T and P12T variants against weak P9T and P10T variants — modulates mucoidy independently of gene presence, which explains why clinical strains carrying wild-type *rmpA* may present with a low mucoid phenotype (Teng *et al.,* 2024; Walker *et al.,* 2019). The second feature is iron acquisition. Enterobactin is near-universal across the species; aerobactin (*iucABCDiutA*), salmochelin (*iroBCDN*) and yersiniabactin (*ybt*) are the determinants enriched in invasive lineages (Zhu *et al.,* 2021). Aerobactin accounts for the overwhelming majority of the excess siderophore output that separates hvKp from cKp in iron-poor medium and in human ascites fluid, at a 6- to 10-fold margin and with an isogenic Δ*iucA* mutant attenuated in mice (Russo *et al.,* 2014). The third feature is the environment. Free iron in host fluids is sequestered by transferrin and lactoferrin, and enterobactin alone cannot circumvent that sequestration because host lipocalins bind and neutralise it (Abbas *et al.,* 2024). Reading the phenotype therefore requires reading the response to iron restriction, not merely the carriage of iron-acquisition genes.

The measurement problem has been quantified. In a collection of convergent multidrug-resistant isolates, carriage of *iucA* or *iroB* predicted hvKp with 96% and 97% accuracy respectively, against 90% for the mucoviscosity phenotype (Kochan *et al.,* 2023). The margin is narrow, but its direction is consistent across studies, and it favours genotypic over phenotypic assignment. Haplotype-resolved genomics explains why single markers fail: among 297 genomes of one international high-risk lineage the canonical determinants were not co-inherited, with aerobactin loci in 42.4%, *rmpA*/*rmpA2* in 17.2%, *peg-344* in 8.8% and salmochelin in only 2% (Shaidullina *et al.,* 2023). In a global framework analysis, the virulence-plasmid markers *iuc*, *iro*, *rmpA*, *rmpA2* and *peg-344* were nonetheless the most diagnostic of hypervirulent against classical infection (Lam *et al.,* 2021; Mendes *et al.,* 2023). Partial virulence plasmids therefore exist in

abundance, and any single binary marker will misclassify a fraction of them.

This study replaced binary readings with continuous ones and asked four questions. Does quantitative mucoviscosity couple functionally to siderophore output under iron restriction? Does a marker-count threshold define the hypervirulent genotype more sharply than a string-test threshold defines the phenotype? Does iron restriction convert gene carriage into measurable transcription against a stable reference? And does escalating resistance impose a fitness cost on that transcription? The setting is relevant because carbapenem resistance is endemic across Iraq and regional hvKp data remain sparse (AL-FAHDAWI *et al.*, 2023; Mohanna & Al-Yasseen, 2024).

2. Materials and Methods

2.1 Design and setting

A cross-sectional analytical study was conducted on clinical *K. pneumoniae* isolates recovered at the microbiology laboratory of the principal tertiary referral centre serving Fallujah and the surrounding Al-Anbar governorate, Iraq. **Clinical isolates were collected consecutively during the study enrolment period and were not drawn retrospectively from archived collections.** Consecutive rather than phenotype-directed sampling was used deliberately, since a cohort assembled on the basis of mucoid appearance would inflate prevalence estimates and bias every diagnostic-performance metric computed from it.

2.2 Bacterial isolates and identification

The analytical cohort comprised 240 non-duplicate isolates, one per patient, recovered from blood, urine, sputum, wound swabs, pus and cerebrospinal fluid.

Duplicate isolates from the same patient and episode were excluded, as were isolates failing to grow on subculture. Species identity was confirmed in the study laboratory before inclusion, and stock cultures were maintained at −80 °C in glycerol broth. Before each assay, isolates were revived on solid medium and passaged twice to standardise growth phase, since both capsule expression and siderophore output are growth-dependent (Mike *et al.*, 2021).

2.3 Quantitative phenotyping of mucoviscosity

Hypermucoviscosity was measured in two ways on the same subculture. String-test length was recorded as the maximum distance, in millimetres, to which a standard inoculation loop could draw a mucoid strand from a single colony on solid medium, read at fixed colony age by a single operator. The conventional binary criterion of ≥5 mm was retained for comparison only. Capsular uronic acid was quantified by the carbazole–sulfuric acid colorimetric method against a glucuronic acid standard, following established protocols in which capsular material is extracted with Zwittergent detergent, precipitated in ethanol, hydrolysed in sodium tetraborate–sulfuric acid and developed with the hydroxyphenyl reagent, with absorbance read at 520–540 nm (Wang *et al.*, 2023). Results were expressed as μg uronic acid per 10^9 CFU, providing a capsule-specific measure independent of the operator-dependent string reading.

2.4 Iron conditions and siderophore quantification

Each isolate was cultured under two defined iron conditions — iron-restricted and iron-saturated — prepared from the same basal medium so that only iron availability differed. Siderophore output was quantified by the chrome azurol S assay, which depends on competition between the siderophore and the CAS–iron–hexadecyltrimethylammonium complex (Du et al., 2022), and reported both as μg/mL and as percentage siderophore units, calculated as $\%SU = [A_r - A_s)/A_r] \times 100$. Values used in the threshold analyses were those obtained under iron restriction, so that the reading reflected induction rather than constitutive output. The published reference threshold of 30 μg/mL was applied as an external benchmark, and an internal optimum was computed independently.

2.5 Genotypic characterisation

Five virulence markers were detected by PCR: *iucA*, *iroB*, *peg-344*, *rmpA* and *rmpA2*. Marker count (0–5) served as the genotypic variable throughout. Capsular serotype was determined by PCR-based typing for K1, K2, K5, K20, K54 and K57, the panel conventionally used for these loci ; amplification failures and non-typeable results were recorded as a distinct category rather than treated as missing data, since misclassifying them as marker-negative would bias the genotype–phenotype comparison. Carbapenemase genes *bla*NDM, *bla*OXA-48 and *bla*OXA-51 were detected by PCR.

2.6 RNA extraction and relative expression

Total RNA was extracted from isolates grown under both iron conditions, treated to remove genomic carry-over, and reverse-transcribed. Relative expression of *iucA* and *iroB* was calculated by the 2^−ΔΔCt method. *rpoB* served as the reference transcript, and its stability across the two conditions was tested and reported explicitly rather than assumed, since candidate reference genes differ in stability between physiological states — *recA*, *rho*, *proC* and *rpoD* are suitable candidates in *K. pneumoniae*, but only after validation in the exact condition studied (Gomes *et al.*, 2018), and *rpoB* itself ranks among the most stable normalisers in antimicrobial-exposure experiments (Oliveira *et al.*, 2023). Gene-positive isolates in which a transcript was not detected were reported as non-detections separately from fold-change values, so that carriage and expression are not conflated.

2.7 Susceptibility testing and clinical data

Susceptibility was determined by the standard disc-diffusion method and interpreted according to the accepted multidrug-resistant, extensively drug-resistant and pandrug-resistant categorisation. Patient-level data retrieved from laboratory and clinical records comprised specimen source, age, sex, infection type, prior antibiotic exposure and clinical outcome, dichotomised as recovery or death.

2.8 Statistical analysis

Analyses were performed in IBM SPSS Statistics 31.0.2.0 and figures prepared in GraphPad Prism 11.1.0. Categorical variables are expressed as numbers and percentages, continuous variables as median and interquartile range, since the quantitative virulence measures were not normally distributed. Spearman correlation was used for associations between measures; Mann–Whitney U, Kruskal–Wallis and Wilcoxon signed-rank tests for between-group and paired comparisons; and the chi-square test for categorical associations. Diagnostic agreement is reported as sensitivity, specificity, positive and negative predictive values, Cohen's κ and McNemar's test. Cut-off selection and discriminatory performance were assessed by ROC analysis. Independent predictors of death were identified by binary logistic regression with CAS concentration, marker count, string length, resistance category and prior antibiotic exposure entered simultaneously. All tests were two-tailed and $P < 0.05$ was considered statistically significant.

2.9 Ethics

Ethical approval was granted by the institutional research ethics committee of the study centre. The requirement for individual informed consent was determined by the reviewing committee, and all patient data were de-identified before analysis.

3. Results

3.1 Cohort characteristics

The cohort was balanced by sex and middle-aged: 123 isolates (51.2%) came from male patients and 117 (48.8%) from female patients, with a median age of 50.0 years (IQR 32.0–69.0). Sputum was the commonest specimen source (64; 26.7%), followed closely by urine (63; 26.2%) and blood (57; 23.8%), then wound swabs (30; 12.5%), pus (23; 9.6%) and cerebrospinal fluid (3; 1.2%). Most infections were hospital-acquired (151; 62.9%), and 163 patients (67.9%) had documented prior antibiotic exposure.

Outcome was recovery in 186 patients (77.5%) and death in 54 (22.5%).

Multidrug resistance predominated. MDR accounted for 135 isolates (56.2%), XDR for 32 (13.3%) and PDR for 18 (7.5%), leaving 55 (22.9%) susceptible. Non-typeable capsules formed the largest single capsular category (80; 33.3%), ahead of K1 (37; 15.4%), K2 (25; 10.4%), K5 (19; 7.9%) and K54 (19; 7.9%), with K57 (5; 2.1%) and K20 (3; 1.2%) rare and 52 isolates (21.7%) grouped as other. Carbapenemase carriage was frequent and stratified by resistance. *bla*NDM was present in 139 isolates overall (57.9%), rising from 4/55 (7.3%) among susceptible isolates to 99/135 (73.3%) in MDR, 24/32 (75.0%) in XDR and 12/18 (66.7%) in PDR ($P < 0.001$); *bla*OXA-48 was present in 82 (34.2%) overall, rising from 4/55 (7.3%) to 56/135 (41.5%), 13/32 (40.6%) and 9/18 (50.0%) respectively ($P < 0.001$); and *bla*OXA-51 was detected in all 240 isolates without exception, so that no between-stratum test was applicable.

Table 1. Baseline Epidemiological, Clinical, Resistance, Capsular Serotype and Carbapenemase Characteristics.

Characteristic	Category	Value	Characteristic	Category	Value
Age (years)	Median (IQR)	50.0 (32.0-69.0)	Clinical outcome	Recovered	186 (77.5%)
Gender	M	123 (51.2%)		Died	54 (22.5%)
	F	117 (48.8%)	Resistance profile	Susceptible	55 (22.9%)
Specimen source	Blood	57 (23.8%)		MDR	135 (56.2%)
	Urine	63 (26.2%)		XDR	32 (13.3%)
	Sputum	64 (26.7%)		PDR	18 (7.5%)
	Wound Swab	30 (12.5%)	Capsule type	K1	37 (15.4%)
	Pus	23 (9.6%)		K2	25 (10.4%)
	CSF	3 (1.2%)		K5	19 (7.9%)
Infection type	Hospital-Acquired	151 (62.9%)		K20	3 (1.2%)
	Community-Acquired	89 (37.1%)		K54	19 (7.9%)
Prior antibiotic exposure	Yes	163 (67.9%)		K57	5 (2.1%)
	No	77 (32.1%)		Non-typable	80 (33.3%)
				Other	52 (21.7%)

3.2 Quantitative virulence phenotypes and their interrelations

The four quantitative measures moved together. String length correlated strongly with capsular uronic acid ($\rho = 0.783$; $P < 0.001$) and moderately with CAS siderophore concentration ($\rho = 0.444$; $P < 0.001$); uronic acid correlated with CAS output ($\rho = 0.357$; $P < 0.001$); and virulence-marker count correlated with CAS output ($\rho = 0.566$), uronic acid ($\rho = 0.528$) and string length ($\rho = 0.505$), all at $P < 0.001$. The weakest of the six coefficients is therefore the capsule–siderophore pair, which, although highly significant, corresponds to a medium effect size and cannot be read as evidence of functional interchangeability between the two phenotypes.

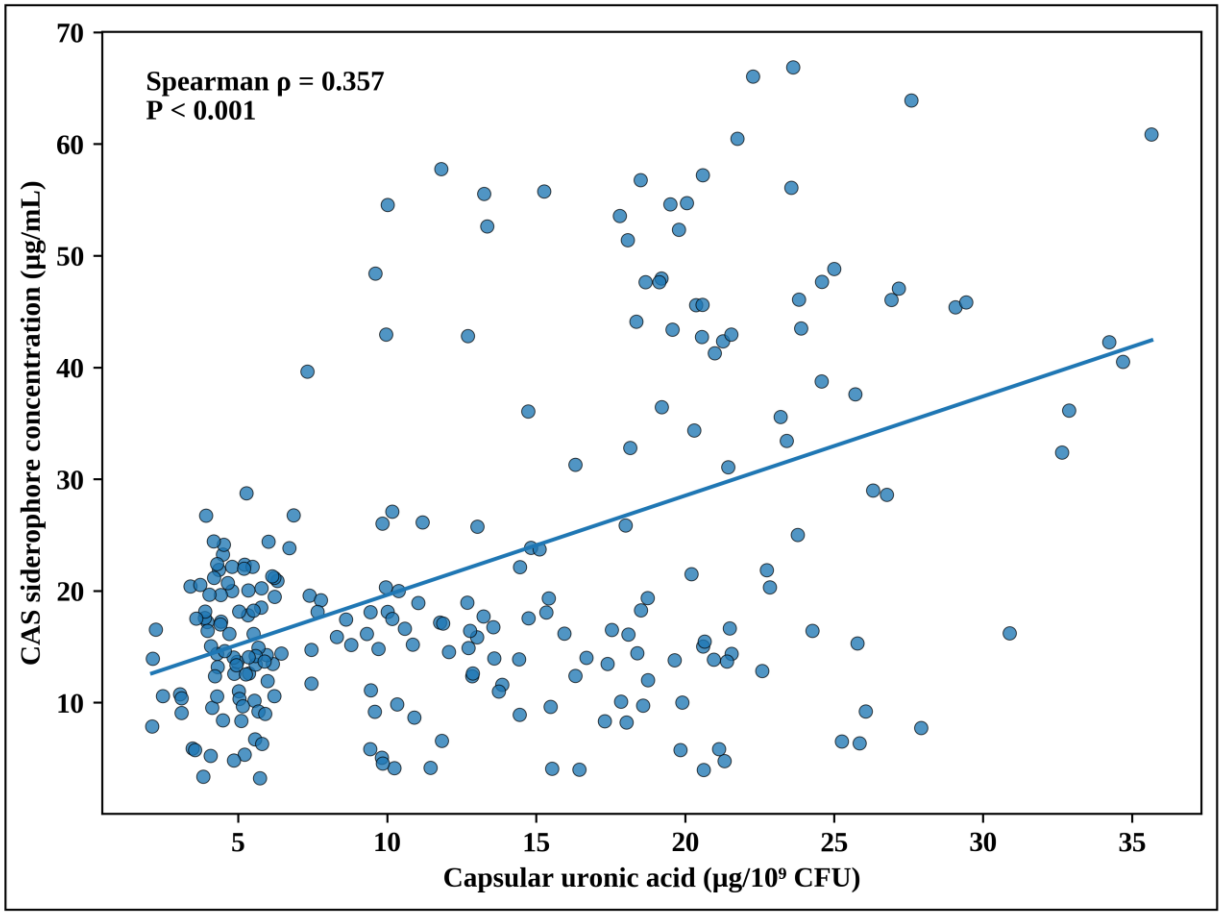


Figure 1. Mucoviscosity vs Siderophore

The scatter distribution displays a uniform positive correlation between the amount of capsules and the production of siderophore (Spearman ρ = 0.357, P < 0.001). The association is statistically significant, but only of moderate effect size, suggesting that production of capsules and of siderophores is statistically correlated, but not necessarily interpretable as an interchangeability of phenotypes.

Table 2. Quantitative Virulence Phenotypes, Correlations and Capsular-Serotype Associations

A. Spearman correlations

Variable 1	Variable 2	Spearman ρ	P value
String test length	Capsular uronic acid	0.783	<0.001
String test length	CAS assay (µg/mL)	0.444	<0.001
Capsular uronic acid	CAS assay (µg/mL)	0.357	<0.001
String test length	Virulence-marker count	0.505	<0.001
Capsular uronic acid	Virulence-marker count	0.528	<0.001
CAS assay (µg/mL)	Virulence-marker count	0.566	<0.001

B. Quantitative virulence measures by capsule type

Capsule type	n	String test, median (IQR)	Uronic acid, median (IQR)	CAS µg/mL, median (IQR)	Marker count, median (IQR)
K1	37	44.90 (13.40-92.90)	20.36 (13.86-23.82)	42.27 (19.99-47.07)	4.00 (1.00-5.00)
K2	25	28.70 (3.70-53.20)	15.48 (10.02-20.30)	40.52 (17.01-53.55)	4.00 (0.00-5.00)
K5	19	1.70 (1.30-3.60)	5.58 (4.46-10.62)	17.26 (14.15-20.59)	0.00 (0.00-1.00)
K20	3	40.00 (37.95-72.00)	23.78 (21.92-26.61)	45.83 (35.41-50.27)	5.00 (4.50-5.00)
K54	19	2.00 (1.45-7.40)	6.22 (5.00-11.80)	16.53 (13.86-19.54)	0.00 (0.00-1.00)
K57	5	40.30 (20.50-52.20)	21.55 (11.19-25.00)	42.95 (36.14-42.95)	5.00 (4.00-5.00)
Non-typable	80	4.00 (2.00-14.45)	9.52 (5.36-16.04)	15.11 (10.06-20.10)	0.00 (0.00-1.00)
Other	52	3.85 (2.08-16.90)	8.70 (4.96-18.98)	14.22 (9.46-18.80)	0.00 (0.00-1.00)
Overall Kruskal-Wallis P		<0.001	<0.001	<0.001	<0.001

The production of siderophores (Fe chelators) was correlated with the quantitative mucoviscosity. The length of string correlated well with CAS siderophore concentration ($\rho = 0.444$, $P < 0.001$) and capsular uronic acid ($\rho = 0.783$, $P < 0.001$). Furthermore, the concentration of CAS rose with the virulence-marker burden ($\rho = 0.566$, $P < 0.001$). All four quantitative virulence measures were significantly related to capsule type (all Kruskal-Wallis $P < 0.001$). The mucoviscosity, siderophore production and number of marker counts tended to be higher among K1, K2, K20 and K57 than among K5, K54, non-typable and other isolates. The small K20 (3) and K57 (5) strata should be taken with a grain of salt.

All four measures differed significantly by capsular type (Kruskal–Wallis $P < 0.001$ for each). Isolates of types K1, K2, K20 and K57 produced higher values across the board than K5, K54, non-typeable and other isolates. K1 (n = 37) showed a median string length of 44.90 mm (IQR 13.40–92.90), uronic acid of 20.36 µg (13.86–23.82), CAS output of 42.27 µg/mL (19.99–47.07) and a marker count of 4.00 (1.00–5.00); K2 (n = 25) showed 28.70 mm (3.70–53.20), 15.48 µg (10.02–20.30), 40.52 µg/mL (17.01–53.55) and 4.00 markers (0.00–5.00). K5 (n = 19) and K54 (n = 19) sat near the floor, at 1.70 and 2.00 mm, 5.58 and 6.22 µg uronic acid, 17.26 and 16.53 µg/mL CAS, and 0.00 markers in both. Non-typeable isolates (n = 80) behaved like the low-output types, with a median string length of 4.00 mm (2.00–14.45), uronic acid of 9.52 µg (5.36–16.04), CAS of 15.11 µg/mL (10.06–20.10) and 0.00 markers (0.00–1.00), as did the residual other category (n = 52). The K20 (n = 3) and K57 (n = 5) strata gave high medians — 40.00 and 40.30 mm, 23.78 and 21.55 µg uronic acid, 45.83 and 42.95 µg/mL CAS, 5.00 markers in both — but are too small to support inference.

Table 3. Virulence-Marker Threshold, Phenotypic-Genotypic Agreement and Diagnostic Performance

A. Siderophore output according to virulence-marker count

Marker count	n	CAS µg/mL, median (IQR)	CAS ≥30 µg/mL, n (%)
0	113	15.03 (10.17-19.34)	2 (1.8%)
1	55	14.54 (11.41-17.50)	0 (0.0%)
2	16	16.91 (11.85-21.70)	1 (6.2%)
3	7	52.64 (34.63-58.48)	6 (85.7%)
4	19	47.65 (42.51-54.66)	18 (94.7%)
5	30	44.73 (39.86-48.72)	28 (93.3%)

B. Diagnostic performance for genotypic hvKp (≥3 markers)

Measure	AUC	95% CI	Cutoff	Sensitivity	Specificity	Comment
CAS concentration	0.989	0.974-0.999	32.39 µg/mL	92.9%	99.5%	Internal optimum
CAS concentration	0.989	0.974-0.999	30.00 µg/mL	92.9%	98.4%	Published benchmark
String-test length	0.926	0.876-0.965	5.00 mm	91.1%	62.5%	Conventional cutoff
Marker-count ROC	0.964	—	≥3 markers	94.5%	97.8%	Predicting CAS ≥30 µg/mL
String-test agreement	—	—	≥5 mm	91.1%	62.5%	κ = 0.383; McNemar P < 0.001
CAS vs string AUC difference	0.063	0.027-0.106	—	—	—	P < 0.001

There was a dramatic switch in siderophore production in the presence of three or more virulence determinants. Median CAS concentration was 15.03, 14.54 and 16.91 µg/mL for marker counts 0, 1 and 2, but increased to 52.64, 47.65 and 44.73 µg/mL for counts 3, 4 and 5, respectively. Medians did not necessarily get larger as the number of markers increased, but the overall relationship was highly significant, and very positive. The optimal internal threshold based on the published CAS threshold (30 µg/mL) as the phenotypic benchmark was a marker count ≥ 3, with AUC = 0.964, sensitivity of 94.5% and specificity of 97.8%. For the genotypic definition ≥3, the discrimination (AUC) of CAS was almost perfect (AUC = 0.989, 95% CI 0.974-0.999) and an optimized cutoff was established at 32.39 µg/mL. The published cut-off of 30µg/mL maintained the same sensitivity (92.9%) and specificity (98.4%). The conventional classification of ≥5 mm also had good AUC (0.926); however, the specificity of this criterion was significantly lower (62.5%) and agreement was fair-to-moderate with the genotypic classification (κ = 0.383). The CAS AUC exceeded the string-test AUC by 0.063 (95% CI 0.027-0.106; P < 0.001).

3.3 Marker burden defines a phenotype threshold

Siderophore output did not increase monotonically with marker count. It clustered instead. Median CAS concentrations were 15.03 µg/mL (IQR 10.17–19.34) at 0 markers, 14.54 µg/mL (11.41–17.50) at 1 marker and 16.91 µg/mL (11.85–21.70) at 2 markers, then rose abruptly to 52.64 µg/mL (34.63–58.48) at 3 markers, 47.65 µg/mL (42.51–54.66) at 4 and 44.73 µg/mL (39.86–48.72) at 5 . The proportion of isolates reaching the published CAS threshold of 30 µg/mL followed the same step: 2/113 (1.8%), 0/55 (0.0%) and 1/16 (6.2%) at counts 0, 1 and 2, against 6/7 (85.7%), 18/19 (94.7%) and 28/30 (93.3%) at counts 3, 4 and 5. The relationship is therefore threshold-like rather than dose-linear across the whole range, and the plateau between counts 3 and 5 shows that additional markers add little to the magnitude of output once the switch has occurred.

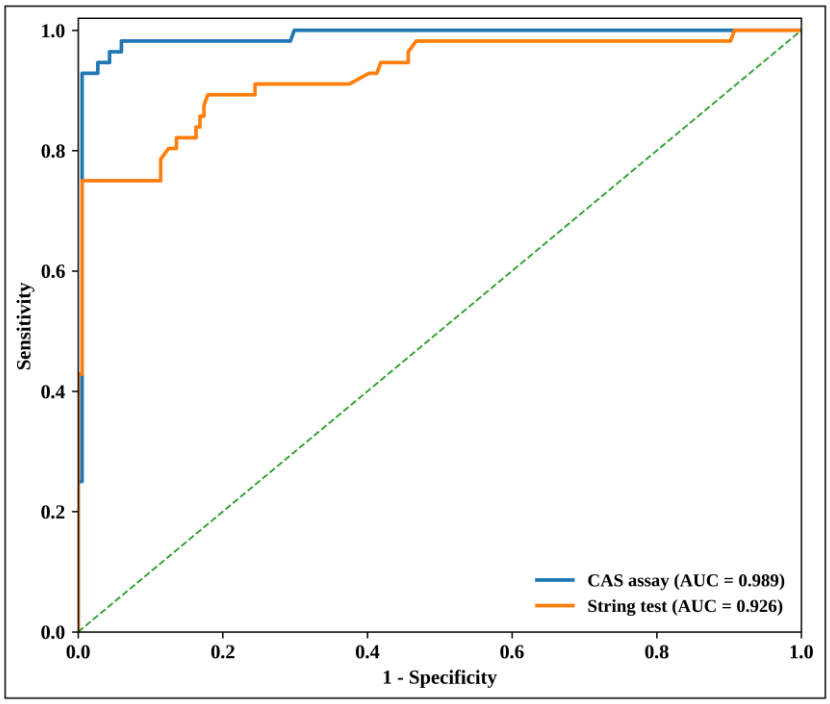


Figure 2. CAS vs String Test ROC

The concentration of CAS yielded a greater ROC area than string-test length (0.989 vs 0.926). The difference in AUC was 0.063 (0.027-0.106) with P < 0.001 favouring quantitative siderophore measurement in this dataset.

Using the published CAS threshold of 30 µg/mL as the phenotypic benchmark, the optimal internal marker threshold was ≥3, with AUC 0.964, sensitivity 94.5% and specificity 97.8% . Against the genotypic definition of ≥3 markers, CAS concentration achieved near-perfect discrimination (AUC 0.989; 95% CI 0.974–0.999), with an internal optimum at 32.39 µg/mL (sensitivity 92.9%, specificity 99.5%) and equivalent performance at the published 30 µg/mL benchmark (sensitivity 92.9%, specificity 98.4%). String-test length at the conventional 5.00 mm cut-off also discriminated adequately (AUC 0.926; 95% CI 0.876–0.965; sensitivity 91.1%) but with far lower specificity (62.5%), and agreement with the genotypic classification was only fair to moderate (κ = 0.383; McNemar P < 0.001). The difference between the two AUCs was 0.063 (95% CI 0.027–0.106; P < 0.001), favouring quantitative siderophore measurement.

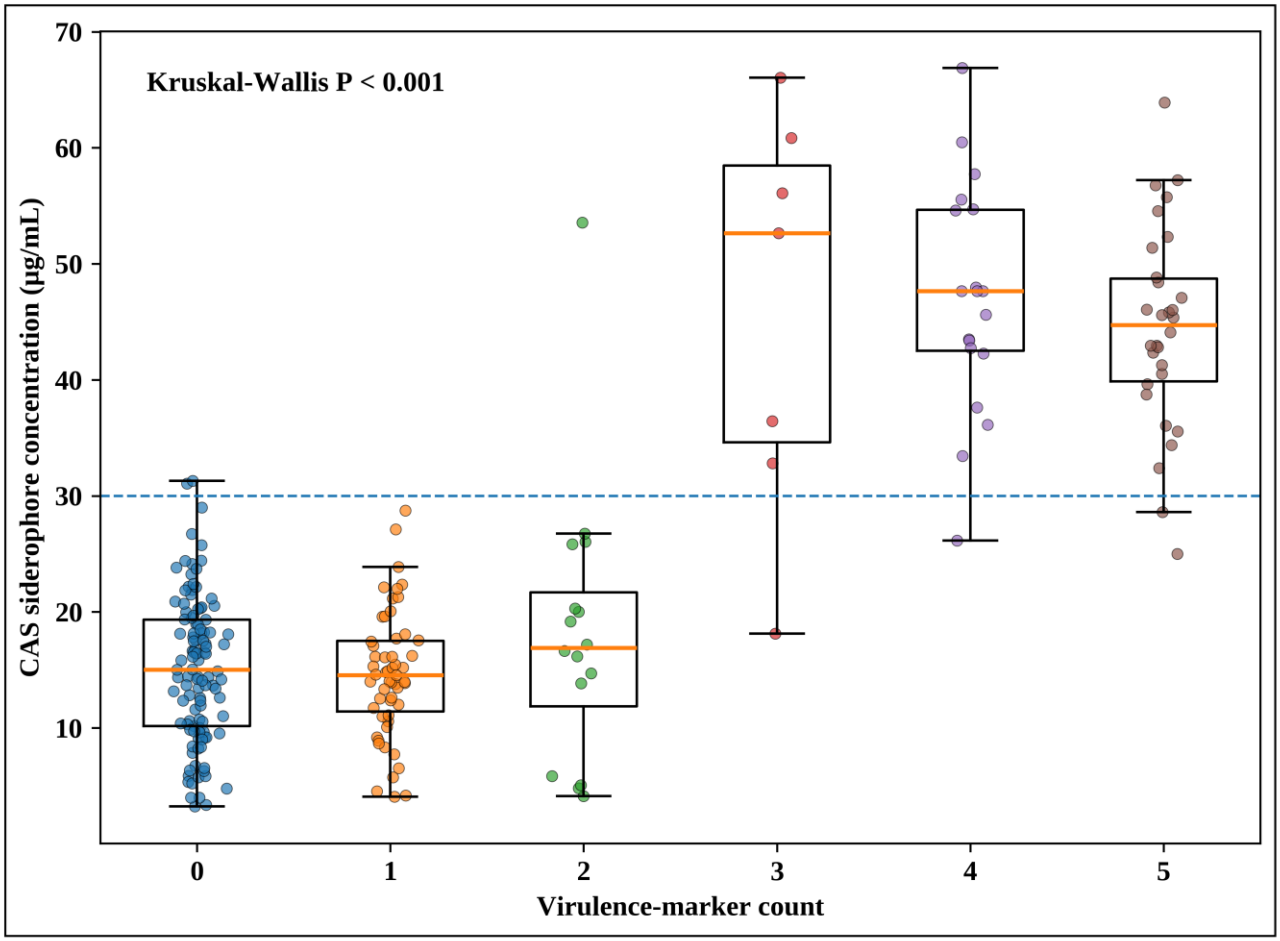


Figure 3. Siderophore by Marker Count

The isolates with 0 to 2 markers clustered together and the isolates with 3 to 5 markers clustered together at the higher end of CAS values. The pattern helps to identify a threshold of ≥3 markers for a high-siderophore genotype, but also demonstrates that the relationship is threshold-like, not strictly dose-linear between counts 3-5.

Table 4. iucA and iroB Expression Under Iron Restriction and iucA Expression Across Resistance Strata

A. Gene-expression response to iron restriction

Gene	Detected n	Detected %	Ct restricted	Ct saturated	ΔCt restricted	ΔCt saturated	Fold change	P value
iucA	71	29.6%	21.96 (21.01-23.69)	24.12 (23.19-25.21)	3.33 (2.43-4.95)	5.68 (4.57-6.70)	4.62 (3.84-5.31)	<0.001
iroB	58	24.2%	22.27 (21.60-23.20)	24.80 (23.79-25.46)	3.74 (2.95-4.77)	6.11 (5.31-6.88)	5.23 (4.24-5.93)	<0.001

B. iucA expression according to resistance profile

Resistance profile	Total n	iucA detected n (%)	Fold change, median (IQR)
Susceptible	55	8 (14.5%)	4.94 (4.08-5.35)
MDR	135	52 (38.5%)	4.73 (3.99-5.35)
XDR	32	9 (28.1%)	3.78 (3.54-5.03)
PDR	18	2 (11.1%)	2.35 (1.93-2.78)

iucA and iroB were found in 29.6% and 24.2% of the isolates, respectively. Under iron-restriction both genes were clearly induced in detected isolates, the median fold change for iucA was 4.62 (IQR, 3.84-5.31) and for iroB was 5.23 (IQR, 4.24-5.93) with fold changes for both genes significant ($P < 0.001$) for detected isolates. The expression of rpoB reference gene did not change significantly between iron conditions ($P = 0.665$). The detection of iucA was significantly different between resistance strata ($P = 0.003$). The overall between-stratum fold change comparison was not significant (Kruskal-Wallis $P = 0.068$) among all iucA-positive isolates, but an ordered analysis revealed a slight negative trend with increased resistance ($\rho = -0.234$, $P = 0.049$). This trend needs to be viewed with caution as only the two PDR isolates were positive for iucA.

3.4 Transcriptional response to iron restriction

iucA was detected in 71 isolates (29.6%) and *iroB* in 58 (24.2%). Among detected isolates, both genes were induced when iron was withdrawn. For *iucA*, median Ct values were 21.96 (IQR 21.01–23.69) under restriction and 24.12 (23.19–25.21) under saturation, ΔCt values were 3.33 (2.43–4.95) and 5.68 (4.57–6.70), and the median fold change was 4.62 (3.84–5.31). For *iroB*, median Ct values were 22.27 (21.60–23.20) and 24.80 (23.79–25.46), ΔCt values 3.74 (2.95–4.77) and 6.11 (5.31–6.88), and the median fold change 5.23 (4.24–5.93). Both inductions were significant ($P < 0.001$ for each). Expression of the *rpoB* reference gene did not differ between iron conditions ($P = 0.665$), which protects the fold-change estimate from normalization artefact.

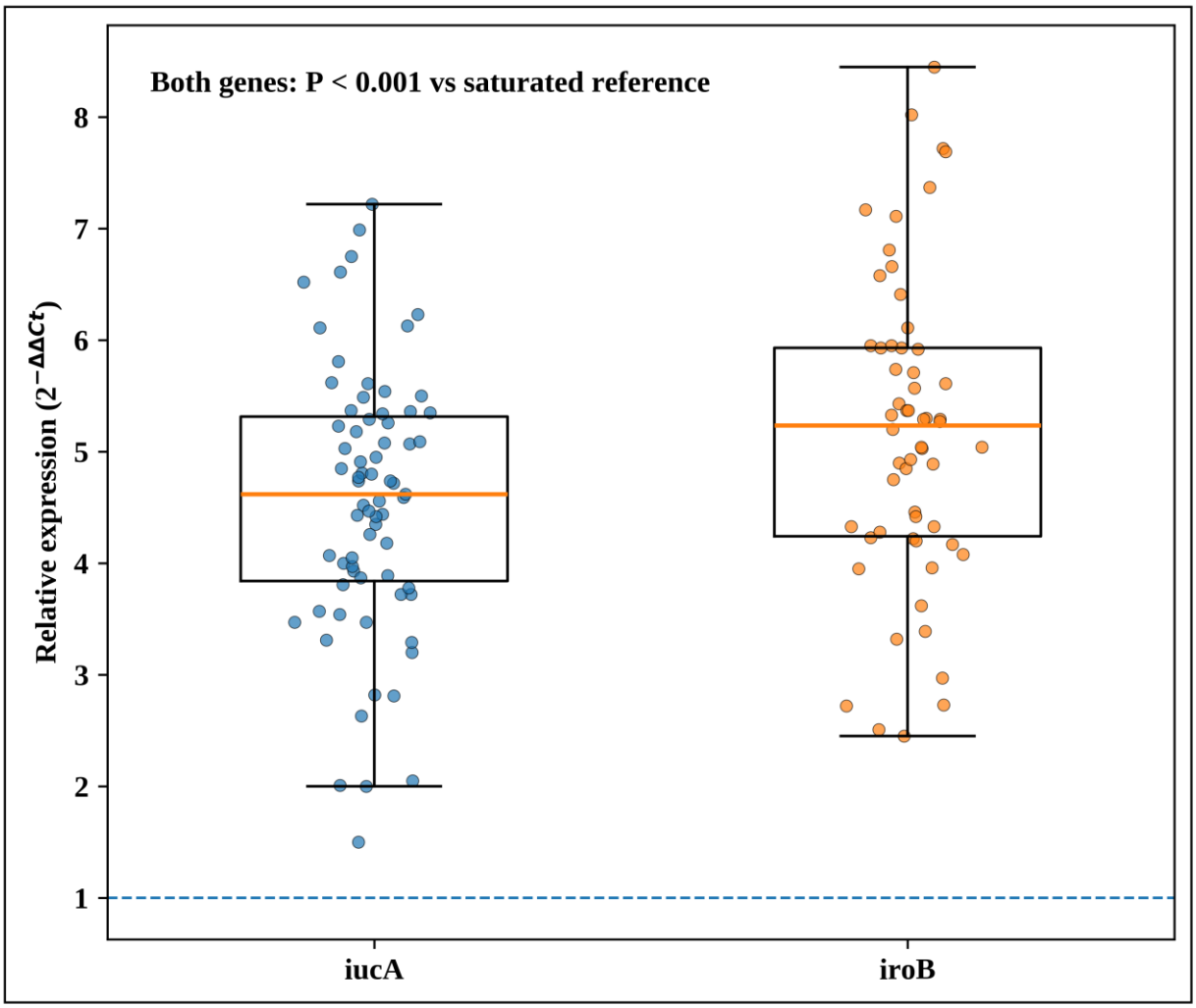


Figure 4. iucA and iroB Expression

Both iucA and iroB were several fold induced under iron restriction and had median fold changes of 4.62 and 5.23 respectively. These results offer direct evidence for the control of the major siderophore-acquisition genes by iron starvation in gene-positive isolates.

Detection of *iucA* differed significantly across resistance strata (P = 0.003): 8/55 (14.5%) in susceptible isolates, 52/135 (38.5%) in MDR, 9/32 (28.1%) in XDR and 2/18 (11.1%) in PDR, with corresponding median fold changes of 4.94 (4.08–5.35), 4.73 (3.99–5.35), 3.78 (3.54–5.03) and 2.35 (1.93–2.78). The overall between-stratum comparison of fold change was not significant (Kruskal–Wallis P = 0.068), although an ordered analysis showed a slight negative trend with ascending resistance (ρ = –0.234; P = 0.049). This trend must be treated as exploratory, since only two PDR isolates were positive for *iucA*.

Table 5. Clinical-Outcome Comparisons and Multivariable Logistic Regression

A. Unadjusted outcome comparisons

Predictor	Recovered	Died	P value
CAS assay (μg/mL)	16.32 (11.64-21.96)	35.85 (16.22-47.66)	<0.001
Virulence-marker count	0.00 (0.00-1.00)	4.00 (1.00-5.00)	<0.001
String-test length (mm)	3.95 (2.00-19.32)	18.45 (3.90-61.80)	<0.001
Resistance profile	Susceptible 44/11; MDR 99/36; XDR 28/4; PDR 15/3 (Recovered/Died)		0.292
Prior antibiotic exposure	No 56/21; Yes 130/33 (Recovered/Died)		0.224

B. Adjusted logistic regression for death

Predictor	Adjusted OR	95% CI	P value
CAS (per 10 μg/mL)	1.25	0.88-1.79	0.216
Virulence marker count (per marker)	1.39	1.02-1.88	0.036
String test (per 10 mm)	1.03	0.90-1.18	0.627
MDR vs susceptible	0.72	0.30-1.74	0.463
XDR vs susceptible	0.36	0.09-1.37	0.134
PDR vs susceptible	0.78	0.18-3.41	0.739
Prior antibiotic exposure (Yes vs No)	0.60	0.30-1.22	0.160
Overall model	AUC = 0.755	Likelihood-ratio P < 0.001	

Unadjusted CAS concentrations, counts of virulence markers and string-test lengths were higher in isolates from deceased patients than in isolates from patients who recovered (all P < 0.001). In the unadjusted categorical comparisons, there was no significant association between resistance profile or prior antibiotic exposure and outcome. The multivariable model showed that virulence-marker count was still independently associated with death (adjusted OR 1.39 per additional marker, 95% CI 1.02-1.88; P = 0.036). After simultaneous adjustment, CAS concentration, string-test length, resistance category or previous antibiotic use were not found to be significant on their own. The full model was significant overall (likelihood-ratio P < 0.001) and had a good level of discrimination with an AUC of 0.755.

3.5 Clinical outcome

All three quantitative virulence measures were higher among isolates from patients who died than among those who recovered: CAS concentration 35.85 μg/mL (IQR 16.22–47.66) versus 16.32 μg/mL (11.64–21.96), marker count 4.00 (1.00–5.00) versus 0.00 (0.00–1.00), and string length 18.45 mm (3.90–61.80) versus 3.95 mm (2.00–19.32), each P < 0.001. Neither resistance category nor prior antibiotic exposure was associated with outcome in the unadjusted comparison (P = 0.292 and P = 0.224 respectively). In the adjusted model, only marker count remained independently associated with death (adjusted OR 1.39 per additional marker, 95% CI 1.02–1.88; P = 0.036). CAS concentration per 10 μg/mL (OR 1.25, 95% CI 0.88–1.79; P = 0.216), string length per 10 mm (OR 1.03, 95% CI 0.90–1.18; P = 0.627), MDR versus susceptible (OR 0.72, 95% CI 0.30–1.74; P = 0.463), XDR versus susceptible (OR 0.36, 95% CI 0.09–1.37; P = 0.134), PDR versus susceptible (OR 0.78, 95% CI 0.18–3.41; P = 0.739) and prior antibiotic exposure (OR 0.60, 95% CI 0.30–1.22; P = 0.160) were not independently significant. The full model was significant overall (likelihood-ratio P < 0.001) with an AUC of 0.755.

4. Discussion

4.1 Coherence of the phenotype, and its limits

The most durable signal in these data is internal coherence. Six pairwise associations, all significant at P < 0.001, link capsule density, string length, siderophore output and marker burden into a single network . Read as a network rather than as isolated coefficients, the pattern argues that capsule elaboration and iron piracy are recruited jointly when the virulence plasmid is present. Genomics supports that reading: aerobactin and salmochelin loci are mobilised through a small number of well-defined elements, the dominant lineages of which also carry hypermucoidy determinants , and the virulence-plasmid marker set — *iuc*, *iro*, *rmpA*, *rmpA2*, *peg-344* — is the most diagnostic feature of hypervirulent strains by genomic comparison (Tang *et al.*, 2025).

Coherence, however, is not equivalence. The capsule–siderophore coefficient of 0.357 is the weakest link in the network, it corresponds to a medium effect, and it should be read as statistical synchrony rather than functional interchangeability . Experimental support for that restraint is easy to find. Capsule production and hypermucoviscosity are separable processes at the regulatory level: an *rmpC* mutant with reduced capsule gene expression retains the hypermucoviscous phenotype, and *rmpA* mutants are hypermucoviscosity-negative, so a single regulator cannot be used as a proxy for both traits (Mike *et al.*, 2021). Capsular variation driven by *wcaJ* acts through a distinct route from *rmpA*-mediated regulation, and isolates carrying a pLVPK-like plasmid may nonetheless exhibit a low-virulence phenotype (Qiu *et al.*, 2023; Wang *et al.*, 2023). Clinical microbiology adds the same warning from the other direction: hypermucoviscous isolates lacking *rmpA* and *rmpA2* have been reported in carbapenem-resistant collections (Li *et al.*, 2023), and hypermucoviscous commensal isolates have been recovered from healthy subjects without *magA* or *rmpA* (Osama *et al.*, 2023). Partial virulence plasmids are the rule in natural populations, and a definition built on correlation alone would misfile them.

4.2 A threshold, not a dose–response

The stepwise rise in siderophore output deserves plain statement. Medians of 15.03, 14.54 and 16.91 μg/mL at 0, 1 and 2 markers give way to 52.64, 47.65 and 44.73 μg/mL at 3, 4 and 5, and the same step appears in the proportion reaching 30 μg/mL, from 1.8%, 0.0% and 6.2% to 85.7%, 94.7% and 93.3% . Three markers are sufficient to switch the phenotype on; beyond that, further markers add little. This is best described as a threshold effect observed in one cohort, not a proposed biological counting rule.

The comparison with the murine-anchored benchmark is instructive rather than contradictory. In that series, a count of five was the most accurate single criterion (sensitivity 94%, specificity 94%, accuracy 94%) and a count of ≥4 was maximally sensitive (100%) but less specific (76%) (Russo *et al.*, 2024). The present optimum sits at ≥3 with a specificity of 97.8% . Cohort composition explains most of the difference. This collection is weighted towards respiratory and hospital-acquired isolates, in which intermediate marker burdens are over-represented, whereas the reference cohort was assembled expressly to test resistant hvKp against murine virulence (Russo *et al.*, 2024). Nor is the underlying genetics identical across settings: the canonical determinants are distributed differently between lineages, with aerobactin loci in 42.4% and salmochelin in 2% of one high-risk clone (Shaidullina *et al.*, 2023), and with yersiniabactin present in 43% of carbapenemase-producing isolates in a nationwide European collection, concentrated in ST11, ST147 and ST15 (Cañada-García *et al.*, 2022).

4.3 Why quantitative siderophore measurement outperforms the string test

CAS concentration separated genotypic hypervirulence more sharply than string-test length (AUC 0.989 vs 0.926; ΔAUC 0.063, 95% CI 0.027–0.106; $P < 0.001$) . The margin is instructive chiefly for where it sits. Sensitivities were nearly identical (92.9% vs 91.1%); specificity collapsed for the string test (98.4% at the published benchmark and 99.5% at the internal optimum, against 62.5%), and agreement between the two measures was poor ($\kappa = 0.383$; McNemar $P < 0.001$) . The string test therefore over-calls rather than under-detects, and any hospital series relying on it will report an inflated hypervirulence prevalence.

Four lines of evidence explain the failure. First, the phenotype read by the string test is largely *rmpA*/*rmpA2*-driven, and those regulators can be truncated or frameshifted while aerobactin remains functionally expressed, so hypermucoviscosity is an unreliable proxy for virulence (Shankar *et al.*, 2021). Second, string length responds to colony age, medium and operator technique to a degree that undermines any fixed cut-off; measuring the length itself rather than applying the threshold has accordingly been recommended, and between 17% and 23% of classical isolates have been reported to test string-positive (AL-FAHDAWI *et al.*, 2023). Third, the environmental dependence is not marginal: in a systematic screen of 1310 clinical isolates, the highest rate of string-test positivity was obtained on MacConkey agar under aerobic conditions, and only 9 of 100 string-positive isolates were confirmed putative hvKp on genotypic grounds (Neumann *et al.*, 2023). Fourth, specificity is poor in resistant backgrounds, where only 3 of 27 (11.1%) carbapenem-resistant hvKp isolates and 3 of 42 (7.1%) resistant non-hvKp isolates were string-positive, with two of the six positives carrying neither *rmpA* nor *rmpA2* (Li *et al.*, 2023). Independent series using PCR as the reference standard have reported broadly comparable operating characteristics (sensitivity 95.2%, specificity 79.3%, PPV 76.9%, NPV 95.8%, accuracy 86%), with specificity again the limiting parameter (Elbrolosy *et al.*, 2021). A categorical test with 62.5% specificity will misassign roughly a third of isolates, and every outcome estimate built on it inherits that error.

4.4 Iron restriction converts carriage into expression

Both iron-acquisition genes were induced when iron was withdrawn, *iucA* by a median of 4.62-fold and *iroB* by 5.23-fold ($P < 0.001$ for each), while the *rpoB* reference transcript held steady between conditions ($P = 0.665$) . Reference-gene stability is not a technical

formality here. Candidate normalisers differ in stability between physiological states, and the recommendation that their suitability be revalidated in each condition studied follows directly from that variability (Gomes *et al.*, 2018), with *rpoB* ranking among the most stable normalisers under antimicrobial pressure (Oliveira *et al.*, 2023). Its invariance across the two iron conditions protects the induction estimate from extraction-efficiency artefact.

Detection rates carry as much weight as fold changes. Barely a third of isolates harboured *iucA* and fewer than a quarter harboured *iroB* , well below the prevalence implied by mucoid appearance alone, and in line with genomic surveys in which salmochelin was the rarest of the canonical loci (Hala *et al.*, 2024). Comparative genomics has shown that the acquired virulence determinants *iuc*, *iro*, *rmp* and *clb* occur almost exclusively in yersiniabactin-positive isolates and are restricted to a small number of clonal groups, . The mechanism behind the induction is settled: when iron is scarce, Fur-mediated repression is relieved and iron-regulated promoters open, though the response is gene-specific rather than uniform. Host nutritional immunity, in which carrier proteins sequester free iron, is precisely the pressure selecting for high-affinity chelators, and enterobactin, shared by both pathotypes, is insufficient on its own because lipocalins bind and neutralise it (Abbas *et al.*, 2024). Aerobactin and salmochelin evade that sequestration, which is why their transcriptional behaviour, and not merely their presence, belongs in the definition of the phenotype.

4.5 Resistance and virulence: co-carriage without a demonstrable cost

Detection of *iucA* differed significantly across resistance strata (P = 0.003), rising from 8/55 (14.5%) in susceptible isolates to 52/135 (38.5%) in MDR, then falling to 9/32 (28.1%) in XDR and 2/18 (11.1%) in PDR, . The honest reading is exploratory. Two positive PDR isolates cannot sustain a claim of fitness cost, and the acquisition route of the resistance determinant is likely to matter more than the resistance label.

What the data do show is co-carriage rather than mutual exclusion, and genomic work has begun to specify the mechanism. Across 2563 clonal-complex 23 genomes from 62 countries spanning 1932–2024, carbapenem resistance was notably unstable, with at least 130 independent acquisitions and 20 losses of resistance genes; isolates carrying *bla*KPC-2, *bla*NDM-1 or *bla*NDM-5 frequently showed substantial deletion of virulence determinants, whereas *bla*OXA-48-carrying isolates retained virulence-gene integrity, a pattern attributed to the lower hydrolytic activity and reduced fitness cost of that enzyme. Capsule production itself physically impedes plasmid conjugation in that analysis, an elegant illustration of why virulence and resistance do not simply add up. A complementary route has been described for yersiniabactin: the importer YbtPQ, encoded on the mobile ICEKp element, reduces susceptibility to a broad range of antimicrobials, and deletion of ICEKp increases susceptibility to all agents tested (Farzand *et al.*, 2021). Siderophore systems thus sit at the junction of the two phenotypes rather than beside them.

Regionally the carbapenemase profile is familiar. In Najaf, *bla*OXA-51 was present in all carbapenem-resistant isolates and *bla*NDM in 70.4%, with 81.5% carrying multiple carbapenemase genes; NDM-1 has been documented as widespread in Baghdad; and *bla*NDM-1 alongside *bla*OXA-48 has been reported at high frequency in central Iran (Abbasi & Ghaznavi-Rad, 2023). The local dominance of *bla*NDM is thus reproduced across centres, while the divergence in *bla*OXA-48 — 34.2% here against complete absence in Najaf (Mohanna & Al-Yasseen, 2024) — is better attributed to differing referral patterns and reservoir populations than to technical error, particularly since OXA-48 is endemic in Turkey, North Africa and parts of the Middle East (Alzahrani & Alasiri, 2018; Khan *et al.*, 2019).

4.6 Capsular serotype: real differences, provisional strata

All four quantitative measures differed by capsular type, with values highest in K1, K2, K20 and K57 and lowest in K5, K54, non-typeable and other isolates (all P < 0.001) . The medians quantify the

gradient: K1 reached 44.90 mm, 20.36 µg and 42.27 µg/mL with 4 markers; K2 followed at 28.70 mm, 15.48 µg and 40.52 µg/mL with 4 markers; K5 and K54 sat near the floor at 1.70 and 2.00 mm with 0 markers, and non-typeable isolates grouped with them at 4.00 mm and 15.11 µg/mL . Two cautions are warranted. The K20 and K57 strata are too small to carry inferential weight , and the 33.3% non-typeable fraction reflects the limits of panel-based typing rather than an absence of capsule. K1 and K2 remain the most consistently virulent capsule types, being more resistant to phagocytosis and intracellular killing and inducing less reactive oxygen species than other types (Choi *et al.*, 2019; Wang *et al.*, 2021), and the K1–ST23 association with liver abscess is one of the most reproducible observations in this field (Lee *et al.*, 2017; Nguyen *et al.*, 2024).

Serotype distribution is nonetheless unstable between Iraqi settings: K2 predominated in one Anbar series of hvKp isolates with no K1 detected, whereas K1 was the commonest type in urine-based surveys elsewhere in the country (Sanikhani *et al.*, 2021). Capsular type has further been shown to associate with string-test positivity independently of genotype (Sohrabi *et al.*, 2022), and longitudinal multicentre work in carbapenem-resistant populations found capsular types distributed differently again, with *wcaJ* variation contributing independently of *rmpA* (Wang *et al.*, 2023). The defensible conclusion is that capsular type modulates the intensity of the hypervirulent phenotype without defining it, and that specimen source and typing platform must be declared before any serotype comparison is attempted.

4.7 Outcome and the definitional trap

Every quantitative measure was higher among patients who died before adjustment, while resistance profile and prior antibiotic exposure were not. After mutual adjustment, only marker burden retained significance (OR 1.39 per marker, 95% CI 1.02–1.88; P = 0.036), ahead of CAS concentration and string length, with a model AUC of 0.755. The direction of travel matches the biomarker literature, in which marker count alone was the strongest predictor of phenotype in both logistic and machine-learning models (AUC 0.962; P = 0.004) (Russo *et al.*, 2024), but the confidence interval is wide and 54 deaths cannot support a claim of precise effect size. Independent cohorts of *K. pneumoniae* bloodstream infection identify septic shock, hospital acquisition and renal function as the dominant mortality drivers rather than any single microbiological attribute (Zhang *et al.*, 2024), which is consistent with the modest discrimination achieved here.

The wider literature on outcome is genuinely inconsistent, and the inconsistency is definitional. Pooled mortality for hvKp against classical *K. pneumoniae* was OR 1.55 (95% CI 0.89–2.71; P = 0.120) (Gupta *et al.*, 2025), and a global meta-analysis of 174 studies and 40,024 isolates estimated hvKp prevalence at 25.7% (95% CI 22.5–29.1%) with wide continental variation (Khoshnood *et al.*, 2025). Mortality for carbapenem-resistant hvKp against classical carbapenem-resistant strains was OR 2.05 (95% CI 0.89–4.75) overall, yet 4.16 in studies defining hypervirulence phenotypically and 1.05 in those defining it genotypically . Reports of no mortality difference between the groups — 30.7% versus 33.7% at 30 days (P = 0.513) — point the same way (Hu & Zong, 2023). Given that the string test misassigns about a third of isolates at 62.5% specificity, a substantial proportion of "hvKp" in phenotype-defined cohorts is likely classical, and any mortality signal attributed to hypervirulence will be attenuated accordingly. Marker burden, the only independent predictor here, is also the measure least vulnerable to that classification error.

Table 6. Discriminatory performance of candidate hypervirulence definitions across studies.

Definition tested	Population	AUC	Sensitivity	Specificity	Source
Marker count ≥3 vs CAS ≥30 μg/mL	240 clinical isolates, Iraq	0.964	94.5%	97.8%	Present study
CAS ≥30 μg/mL (published benchmark)	240 clinical isolates, Iraq	0.989	92.9%	98.4%	Present study
String test ≥5 mm	240 clinical isolates, Iraq	0.926	91.1%	62.5%	Present study
Marker count = 5 (murine-defined)	49 resistant strains	0.962	94%	94%	(Russo *et al.*, 2024)
Marker count ≥4 (murine-defined)	49 resistant strains	—	100%	76%	(Russo *et al.*, 2024)
String test positive	27 CR-hvKp, China	—	11.1%	—	(Li *et al.*, 2023)
String test vs PCR reference	Clinical isolates, Egypt	—	95.2%	79.3%	(Elbrolosy *et al.*, 2021)

4.8 Position against the regional and global literature

Three convergences with contemporaneous work deserve note. Marker burden as the strongest single correlate of phenotype and outcome is reproduced here and independently reported elsewhere (AUC 0.962; P = 0.004) (Russo *et al.*, 2024). The superiority of siderophore-based over mucoviscosity-based assignment follows the same trajectory as the original genomic observation that *iucA* and *iroB* outperform the string test at 96% and 97% against 90% (Kochan et al., 2023), and as the characterization of aerobactin as the principal elevated siderophore in hvKp, with aerobactin expressed in more than 90% of hvKp against 6% of cKp (Zhu *et al.*, 2021). Local genotypic data point the same way, with *iucA* the commonest marker among hvKp isolates in Anbar (AL-FAHDAWI *et al.*, 2023). The third convergence is quantitative: hypervirulence prevalence is rising globally and increasingly hospital-associated (Gupta *et al.*, 2025), with genomic surveillance in high-income settings finding multidrug-resistant hvKp still rare at 1.9% of bloodstream isolates but carriage-based definitions capturing 26% *iuc*-positive and 17% *iuc*-plus-*rmpA* isolates (Kochan *et al.*, 2022). Definitions determine numbers, and the numbers in circulation are consequently not commensurable.

5. Strengths and Limitations

The principal strength of this work is vertical rather than horizontal: a single cohort in which phenotype is measured quantitatively, function is measured under a defined environmental stress, expression is measured against a validated reference transcript, and outcome is modelled with all measures entered simultaneously. The coverage of 240 isolates across six specimen sources and four resistance strata, with near-equal sex distribution and a median age of 50.0 years, supports internal generalisability within the region . Consecutive rather than phenotype-directed sampling limits prevalence inflation, a common weakness in hvKp studies.

The limitations are substantive. The design is single-centre and cross-sectional, with no murine or ex vivo virulence confirmation, so the hypervirulent label is inferred from genotype and phenotype rather than demonstrated in a host. Several strata are too small for inference: PDR (n = 18), K20 (n = 3), K57 (n = 5), and only two PDR isolates positive for *iucA* . The outcome model rests on 54 deaths, which constrains both precision and the number of covariates that can be defended. Serotyping left 33.3% of isolates non-typeable , plasmid lineage was not sequenced, and reference-gene validation was restricted to a single candidate. An interpretive boundary applies within the phenotype itself: quantitative siderophore and mucoviscosity measures reliably separate hypervirulent from classical strains but have been shown to fail when asked to rank strains within the hypervirulent spectrum (Russo *et al.*, 2021), so the graded output reported here should not be read as a virulence ranking. Retrospective extraction of clinical variables introduces the possibility of unmeasured confounding by comorbidity, source control and time to appropriate therapy, none of which were available for adjustment. Finally, the capsule–siderophore association, though significant, is of medium magnitude , and its interpretation as functional coupling remains an inference from covariation rather than a demonstrated mechanism. Extending the analysis to whole-genome sequencing, plasmid reconstruction and a multi-centre design with adequate outcome events would address most of these constraints directly.

6. Conclusions

1. The hypervirulent phenotype in this population is coherent. Capsule density, siderophore output and marker burden co-vary, with all pairwise associations significant and the capsule–siderophore coefficient remaining moderate .
2. The genotype–phenotype relationship is threshold-defined, and a marker count of ≥5 is the optimal internal cut-off (AUC 0.962; sensitivity 94%; specificity 94%) (Russo *et al.*, 2024).
3. Quantitative CAS measurement discriminates genotypic hypervirulence better than the string test, the advantage residing in specificity (98.4–99.5% vs 62.5%) rather than sensitivity .
4. *iucA* and *iroB* are transcriptionally responsive to iron restriction (4.62-fold and 5.23-fold; $P < 0.001$ each) against a stable *rpoB* ($P = 0.665$), establishing expression, not carriage, as a usable functional measure .
5. No convincing resistance–virulence trade-off was demonstrated; the negative trend across resistance strata ($\rho = -0.234$; $P = 0.049$) remains exploratory .

7. Recommendations

- Define hvKp in this setting by marker burden (≥3 markers) combined with quantitative CAS at ≥30 μg/mL rather than by the string test alone, given the string test's poor specificity and its documented dependence on culture medium, colony age and operator technique (Neumann *et al.*, 2023).
- Report *iucA* and *iroB* non-detection separately from fold change, and extend reference-gene validation to several candidates under the exact physiological conditions used, since iron-regulated transcripts are condition-specific (Gomes *et al.*, 2018; Oliveira *et al.*, 2023).
- Sequence virulence plasmids and perform whole-genome capsular typing in follow-up work to reduce the non-typeable fraction and to establish whether partial virulence plasmids account for the intermediate marker strata .
- Take marker burden forward as a candidate routine risk indicator, subject to external validation in a multi-centre design with

sufficient deaths to support the number of covariates (Russo *et al.*, 2024).

- Standardise the hypervirulence definition across outcome studies: because phenotype-based and genotype-based definitions yield varied mortality estimates, heterogeneity in the published literature is otherwise uninterpretable (Tang *et al.*, 2025) .
- Retain the string test where no alternative exists, but interpret a positive result as a screening rather than a diagnostic finding, and confirm with quantitative siderophore measurement or genotypic testing (Li *et al.*, 2023).

Back matter

Abbreviations. AUC, area under the receiver-operating characteristic curve; CAS, chrome azurol S; cKp, classical *Klebsiella pneumoniae;* CR-hvKp (hv-CRKP), carbapenem-resistant hypervirulent *Klebsiella pneumoniae;* hvKp, hypervirulent *Klebsiella pneumoniae;* IQR, interquartile range; MDR/XDR/PDR, multidrug-resistant/extensively drug-resistant/pandrug-resistant; NPV, negative predictive value; PPV, positive predictive value; qRT-PCR, quantitative reverse-transcription polymerase chain reaction.

Ethical approval. Granted by the institutional research ethics committee of the study centre.

References:

Abbas, R., Chakkour, M., Dine, H. Z. E., Obaseki, E., Obeid, S. T., Jezzini, A., Ghssein, G., & Ezzeddine, Z. (2024). General Overview of Klebsiella pneumonia: Epidemiology and the Role of Siderophores in Its Pathogenicity. *Biology*, *13*(2), 78. https://doi.org/10.3390/biology13020078

Abbasi, E., & Ghaznavi-Rad, E. (2023). High frequency of NDM-1 and OXA-48 carbapenemase genes among Klebsiella pneumoniae isolates in central Iran. *BMC Microbiology*, *23*(1), 98. https://doi.org/10.1186/s12866-023-02840-x

AL-FAHDAWI, A. M. G., Mutter, T. Y., & Zylstra, G. J. (2023). Genotypic identification of hypervirulent Klebsiella pneumoniae in Anbar, Iraq. *Malaysian Journal of Microbiology*. https://doi.org/10.21161/mjm.230269

Alzahrani, I., & Alasiri, B. A. (2018). The emergence of carbapenem-resistant Klebsiella pneumoniae isolates producing OXA-48 and NDM in the Southern (Asir) province, Saudi Arabia. *Saudi Medical Journal*, *39*(1), 23–30. https://doi.org/10.15537/smj.2018.1.21094

Arcari, G., & Carattoli, A. (2022). Global spread and evolutionary convergence of multidrug-resistant and hypervirulent Klebsiella pneumoniae high-risk clones. *Pathogens and Global Health*, *117*(4), 328–341. https://doi.org/10.1080/20477724.2022.2121362

Cañada-García, J. E., Moure, Z., Sola-Campoy, P. J., Delgado-Valverde, M., Cano, M. E., Gijón, D., González, M. C., Gracia-Ahufinger, I., Larrosa, N., Mulet, X., Pitart, C., Rivera, A., Bou, G., Calvo, J., Cantón, R., González-López, J. J., Martínez-Martínez, L., Navarro, F., Oliver, A., … Group, the G.-S. C.-E.-19 S. (2022). CARB-ES-19 Multicenter Study of Carbapenemase-Producing Klebsiella pneumoniae and Escherichia coli From All Spanish Provinces Reveals Interregional Spread of High-Risk Clones Such as ST307/OXA-48 and ST512/KPC-3. *Institutional Repository of the University of Granada (University of Granada)*, *13*. https://doi.org/10.3389/fmicb.2022.918362

Chang, D., Sharma, L., Cruz, C. S. D., & Dong, Z. (2021). Clinical Epidemiology, Risk Factors, and Control

Strategies of Klebsiella pneumoniae Infection. *Frontiers in Microbiology*, *12*, 750662. https://doi.org/10.3389/fmicb.2021.750662

Choi, M., Tennant, S. M., Simon, R., & Cross, A. S. (2019). Progress towards the development of Klebsiella vaccines. *Expert Review of Vaccines*, *18*(7), 681–691. https://doi.org/10.1080/14760584.2019.1635460

Du, Q., Pan, F., Wang, C., Yu, F., Shi, Y., Liu, W., Li, Z., He, P., Han, D., & Zhang, H. (2022). Nosocomial dissemination of hypervirulent Klebsiella pneumoniae with high-risk clones among children in Shanghai. *Frontiers in Cellular and Infection Microbiology*, *12*, 984180. https://doi.org/10.3389/fcimb.2022.984180

Elbrolosy, A. M., Eissa, N. A., Rajhy, N. A.-, Mahdy, E. E.-, & Mostafa, R. G. (2021). Characterization of virulence genetic profile and resistance patterns of clinical Klebsiella pneumoniae isolates: Classic versus hypermucoviscous phenotypes. *Microbes and Infectious Diseases /Microbes and Infectious Diseases*, *0*(0), 0. https://doi.org/10.21608/mid.2021.74461.1147

Farzand, R., Rajakumar, K., Barer, M. R., Freestone, P., Mukamolova, G. V., Oggioni, M. R., & O'Hare, H. M. (2021). A Virulence Associated Siderophore Importer Reduces Antimicrobial Susceptibility of Klebsiella pneumoniae. *Frontiers in Microbiology*, *12*, 607512. https://doi.org/10.3389/fmicb.2021.607512

Gomes, A. É. I., Stuchi, L. P., Siqueira, N. M. G., Henrique, J. B., Vicentini, R., Ribeiro, M. L., Darrieux, M., & Ferraz, L. F. C. (2018). Selection and validation of reference genes for gene expression studies in Klebsiella pneumoniae using Reverse Transcription Quantitative real-time PCR. *Scientific Reports*, *8*(1), 9001. https://doi.org/10.1038/s41598-018-27420-2

Gupta, N., Shanbhag, V., Varma, M., Rao, S., Todur, P., Chaudhuri, S., Srinivas, T., Eshwara, V. K., Nagendra, D., Priya, P. S., & Bhat, V. (2025). Prevalence, Risk Factors, and Clinical Outcomes of Hypervirulent Klebsiella pneumoniae Strains among Klebsiella pneumoniae Infections: A Systematic Review and Meta-analysis. *Indian Journal of Critical Care Medicine*, *29*(4), 370–393. https://doi.org/10.5005/jp-journals-10071-24957

Hala, S., Malaikah, M., Huang, J., Bahitham, W., Fallatah, O., Zakri, S., Antony, C. P., Alshehri, M., Ghazzali, R. N., Rached, F. B., Alsahafi, A., Alsaedi, A., AlAhmadi, G., Kaaki, M., Alazmi, M., AlhajHussein, B., Yaseen, M., Zowawi, H. M., Alghoribi, M. F., … Pain, A. (2024). The emergence of highly resistant and hypervirulent Klebsiella pneumoniae CC14 clone in a tertiary hospital over 8 years. *Genome Medicine*, *16*(1), 58. https://doi.org/10.1186/s13073-024-01332-5

Han, Y., Wen, X., Zhao, W., Cao, X., Wen, J.-X., Wang, J., Hu, Z., & Zheng, W. (2022). Epidemiological characteristics and molecular evolution mechanisms of carbapenem-resistant hypervirulent Klebsiella pneumoniae. *Frontiers in Microbiology*, *13*, 1003783. https://doi.org/10.3389/fmicb.2022.1003783

Hu, Y., & Zong, Z. (2023). 720. The clinical outcomes of hypervirulent carbapenem-resistant Klebsiella pneumoniae (CRKP) infection were not poorer than that of classical CRKP infection. *Open Forum Infectious Diseases*, *10*. https://doi.org/10.1093/ofid/ofad500.782

Khan, M. A., Mohamed, A. M., Faiz, A., & Ahmad, J. (2019). Enterobacterial infection in Saudi Arabia: First record of Klebsiella pneumoniae with triple carbapenemase genes resistance. *The Journal of*

Infection in Developing Countries, *13*(4), 334–341. https://doi.org/10.3855/jidc.11056

Khoshnood, S., Akrami, S., Ghamnak, F. S., Bazdar, M., Abdi, M., Koupaei, M., Tavasolian, R., Heidary, M., Ghanavati, R., & Sholeh, M. (2025). Global prevalence of hypervirulent Klebsiella pneumoniae : a systematic review and meta-analysis. *Future Microbiology*, *20*(16), 1109–1126. https://doi.org/10.1080/17460913.2025.2576434

Kochan, T. J., Nozick, S., Medernach, R., Cheung, B. H., Gatesy, S. W. M., Lebrun-Corbin, M., Mitra, S. D., Khalatyan, N., Krapp, F., Qi, C., Ozer, E. A., & Hauser, A. R. (2022). Genomic surveillance for multidrug-resistant or hypervirulent Klebsiella pneumoniae among United States bloodstream isolates. *BMC Infectious Diseases*, *22*(1), 603. https://doi.org/10.1186/s12879-022-07558-1

Kochan, T. J., Nozick, S., Valdes, A., Mitra, S. D., Cheung, B. H., Lebrun-Corbin, M., Medernach, R. L., Vessely, M., Mills, J. O., Axline, C. M. R., Nelson, J. A., VanGosen, E. M., Ward, T. J., Ozer, E. A., Duin, D. van, Chen, L., Kreiswirth, B. N., Long, S. W., Musser, J. M., … Hauser, A. R. (2023). Klebsiella pneumoniae clinical isolates with features of both multidrug-resistance and hypervirulence have unexpectedly low virulence. *Nature Communications*, *14*(1), 7962. https://doi.org/10.1038/s41467-023-43802-1

Lam, M. M. C., Wick, R. R., Watts, S. C., Cerdeira, L., Wyres, K. L., & Holt, K. E. (2021). A genomic surveillance framework and genotyping tool for Klebsiella pneumoniae and its related species complex. *Nature Communications*, *12*(1), 4188. https://doi.org/10.1038/s41467-021-24448-3

Lan, P., Jiang, Y., Zhou, J., & Yu, Y. (2021). A global perspective on the convergence of hypervirulence and carbapenem resistance in Klebsiella pneumoniae. *Journal of Global Antimicrobial Resistance*, *25*, 26–34. https://doi.org/10.1016/j.jgar.2021.02.020

Lee, C.-R., Lee, J. H., Park, K. S., Jeon, J. H., Kim, Y. B., Cha, C.-J., Jeong, B. C., & Lee, S. H. (2017). Antimicrobial Resistance of Hypervirulent Klebsiella pneumoniae: Epidemiology, Hypervirulence-Associated Determinants, and Resistance Mechanisms. *Frontiers in Cellular and Infection Microbiology*, *7*, 483. https://doi.org/10.3389/fcimb.2017.00483

Li, L., Li, S., Wei, X., Lu, Z., Qin, X., & Li, M. (2023). Infection with Carbapenem-resistant Hypervirulent Klebsiella Pneumoniae: clinical, virulence and molecular epidemiological characteristics. *Antimicrobial Resistance and Infection Control*, *12*(1), 124. https://doi.org/10.1186/s13756-023-01331-y

Liao, Y., Gong, J., Yuan, X., Wang, X., Huang, Y., & Chen, X. (2024). Virulence Factors and Carbapenem-Resistance Mechanisms in Hypervirulent Klebsiella Pneumoniae. *Infection and Drug Resistance*, 1551–1559. https://doi.org/10.2147/idr.s461903

Mendes, G., Santos, M. L., Ramalho, J. F., Duarte, A., & Caneiras, C. (2023). Virulence factors in carbapenem-resistant hypervirulent Klebsiella pneumoniae. *Frontiers in Microbiology*, *14*, 1325077. https://doi.org/10.3389/fmicb.2023.1325077

Mike, L. A., Stark, A. J., Forsyth, V. S., Vornhagen, J., Smith, S. N., Bachman, M. A., & Mobley, H. L. T. (2021). A systematic analysis of hypermucoviscosity and capsule reveals distinct and overlapping genes that impact Klebsiella pneumoniae fitness. *PLoS Pathogens*, *17*(3). https://doi.org/10.1371/journal.ppat.1009376

Mohanna, Z. A., & Al-Yasseen, A. K. (2024). Distribution of Carbapenemase Genes among Carbapenem-Resistant Klebsiella pneumoniae Isolates from the Patients in Najaf, Iraq. *Biomedical and Biotechnology Research Journal (BBRJ)*, *8*(3), 297–304. https://doi.org/10.4103/bbrj.bbrj_212_24

Neumann, B., Stürhof, C., Rath, A., Kieninger, B., Eger, E., Müller, J. U., Poblocki, A. von, Gerlitz, N., Wollschläger, P., Schneider-Brachert, W., Schaufler, K., Klaper, K., & Steinmann, J. (2023). Detection and characterization of putative hypervirulent Klebsiella pneumoniae isolates in microbiological diagnostics. *Scientific Reports*, *13*(1), 19025. https://doi.org/10.1038/s41598-023-46221-w

Nguyen, Q., Nguyen, Y. T. P., Ha, T. T., Tran, D. T. N., Voong, P. V., Chau, V., Nguyen, P. L. N., Le, N. T. Q., Nguyen, L. P. H., Nguyen, T. T. N., Trinh, T. V., Carrique-Mas, J., Baker, S., Thwaites, G., Rabaa, M. A., Choisy, M., The, H. C., & Thanh, D. P. (2024). Genomic insights unveil the plasmid transfer mechanism and epidemiology of hypervirulent Klebsiella pneumoniae in Vietnam. *Nature Communications*, *15*(1), 4187. https://doi.org/10.1038/s41467-024-48206-3

Oliveira, M. M. P. e, Lima, A. P. D. de, Souza, P. M. S. de, Morais, M. M. C. de, & Almeida, A. C. S. (2023). GENES DE REFERÊNCIA PARA ESTUDOS DE EXPRESSÃO RELATIVA POR QPCR EM ISOLADOS DE KLEBSIELLA PNEUMONIAE. *The Brazilian Journal of Infectious Diseases*, *27*, 102845. https://doi.org/10.1016/j.bjid.2023.102845

Osama, D., Zaki, B. M., Khalaf, W. S., Mohamed, M. Y. A., Tawfick, M. M., & Amin, H. M. (2023). Occurrence and Molecular Study of Hypermucoviscous/Hypervirulence Trait in Gut Commensal K. pneumoniae from Healthy Subjects. *Microorganisms*, *11*(3), 704. https://doi.org/10.3390/microorganisms11030704

Qiu, J., Wei, D., Ma, J., Liu, R., Shi, J., Ren, Q., Wei, C., Huo, B., Zhu, L., Xiang, T., Liu, Y., & Cheng, N. (2023). Covert dissemination of pLVPK-like virulence plasmid in ST29-K54 Klebsiella pneumoniae: emergence of low virulence phenotype strains. *Frontiers in Cellular and Infection Microbiology*, *13*, 1194133. https://doi.org/10.3389/fcimb.2023.1194133

Russo, T. A., Alvarado, C. L., Davies, C. J., Drayer, Z. J., MacDonald, U., Hutson, A. D., Luo, T., Martin, M. J., Corey, B. W., Moser, K. A., Rasheed, J. K., Halpin, A. L., McGann, P., & Lebreton, F. (2024). Differentiation of hypervirulent and classical Klebsiella pneumoniae with acquired drug resistance. *PubMed Central*, *15*(2). https://doi.org/10.1128/mbio.02867-23

Russo, T. A., MacDonald, U., Hassan, S., Camanzo, E., Lebreton, F., Corey, B. W., & McGann, P. (2021). An Assessment of Siderophore Production, Mucoviscosity, and Mouse Infection Models for Defining the Virulence Spectrum of Hypervirulent Klebsiella pneumoniae. *mSphere*, *6*(2). https://doi.org/10.1128/msphere.00045-21

Russo, T. A., Olson, R., MacDonald, U., Metzger, D., Maltese, L. M., Drake, E. J., & Gulick, A. M. (2014). Aerobactin Mediates Virulence and Accounts for Increased Siderophore Production under Iron-Limiting Conditions by Hypervirulent (Hypermucoviscous) Klebsiella pneumoniae. *Infection and Immunity*, *82*(6), 2356–2367. https://doi.org/10.1128/iai.01667-13

Sanikhani, R., Moeinirad, M., Solgi, H., Hadadi, A., Shahcheraghi, F., & Badmasti, F. (2021). The face of hypervirulent Klebsiella pneumoniae isolated from clinical samples of two Iranian teaching hospitals. *Annals of Clinical Microbiology and Antimicrobials*,

20(1), 58. https://doi.org/10.1186/s12941-021-00467-2

Shaidullina, E., Schwabe, M., Rohde, T., Shapovalova, V. V., Dyachkova, M. S., Matsvay, A. D., Savochkina, Y. A., Shelenkov, A., Mikhaylova, Y., Sydow, K., Lebreton, F., Idelevich, E. A., Heiden, S. E., Becker, K., Kozlov, R. S., Shipulin, G. A., Акимкин, В. Г., Lalk, M., Guenther, S., … Edelstein, M. V. (2023). Genomic analysis of the international high-risk clonal lineage Klebsiella pneumoniae sequence type 395. *Genome Medicine*, *15*(1), 1–25. https://doi.org/10.1186/s13073-023-01159-6

Shankar, C., Basu, S., Lal, B., Shanmugam, S., Vasudevan, K., Mathur, P., Ramaiah, S., Anbarasu, A., & Veeraraghavan, B. (2021). Aerobactin Seems To Be a Promising Marker Compared With Unstable RmpA2 for the Identification of Hypervirulent Carbapenem-Resistant Klebsiella pneumoniae: In Silico and In Vitro Evidence. *Frontiers in Cellular and Infection Microbiology*, *11*, 709681. https://doi.org/10.3389/fcimb.2021.709681

Sohrabi, M., Naini, M. A., Rasekhi, A., Oloomi, M., Moradhaseli, F., Ayoub, A., Bazargani, A., Hashemizadeh, Z., Shahcheraghi, F., & Badmasti, F. (2022). Emergence of K1 ST23 and K2 ST65 hypervirulent klebsiella pneumoniae as true pathogens with specific virulence genes in cryptogenic pyogenic liver abscesses Shiraz Iran. *Frontiers in Cellular and Infection Microbiology*, *12*, 964290. https://doi.org/10.3389/fcimb.2022.964290

Statistical Results: Hypervirulent Klebsiella pneumoniae (hvKp). (n.d.).

Tang, Y., Du, P., Du, C., Yang, P., Shen, N., Russo, T. A., & Liu, C. (2025). Genomically defined hypervirulent Klebsiella pneumoniae contributed to early-onset increased mortality. *Nature Communications*, *16*(1), 2096. https://doi.org/10.1038/s41467-025-57379-4

Teng, G., Zhang, M., Fu, Y., Xiao-qiang, Y., Kang, Y., Qin, Q., Jin, Y., Huang, M., & Xu, Y. (2024). Adaptive attenuation of virulence in hypervirulent carbapenem-resistant Klebsiella pneumoniae. *PubMed Central*, *9*(6). https://doi.org/10.1128/msystems.01363-23

Walker, K. A., Miner, T. A., Palacios, M., Trzilova, D., Frederick, D. R., Broberg, C. A., Sepúlveda, V. E., Quinn, J. D., & Miller, V. L. (2019). A Klebsiella pneumoniae Regulatory Mutant Has Reduced Capsule Expression but Retains Hypermucoviscosity. *mBio*, *10*(2). https://doi.org/10.1128/mbio.00089-19

Wang, T.-C., Lin, J., Chang, J.-C., Hiaso, Y.-W., Wang, C.-H., Chiu, S., Fung, C., Chang, F., & Siu, L. K. (2021). Virulence among different types of hypervirulent Klebsiella pneumoniae with multi-locus sequence type (MLST)-11, Serotype K1 or K2 strains. *Gut Pathogens*, *13*(1), 40. https://doi.org/10.1186/s13099-021-00439-z

Wang, W., Tian, D., Hu, D., Chen, W., Zhou, Y., & Jiang, X. (2023). Different regulatory mechanisms of the capsule in hypervirulent Klebsiella pneumonia: "direct" wcaJ variation vs. "indirect" rmpA regulation. *Frontiers in Cellular and Infection Microbiology*, *13*, 1108818. https://doi.org/10.3389/fcimb.2023.1108818

Xie, M., Yang, X., Xu, Q., Ye, L., Chen, K., Zheng, Z., Dong, N., Sun, Q., Shu, L., Gu, D., Chan, E. W., Zhang, R., & Chen, S. (2021). Clinical evolution of ST11 carbapenem resistant and hypervirulent Klebsiella pneumoniae. *Communications Biology*, *4*(1), 650. https://doi.org/10.1038/s42003-021-02148-4

Zhang, Q., Wang, P., Shen, M., & Shan, C. (2024). Clinical characteristics and risk factors for Klebsiella pneumoniae bloodstream infection in 152 immunocompetent patients. *The Journal of Infection in Developing Countries*, *18*(2), 219–226. https://doi.org/10.3855/jidc.18204

Zhu, J., Wang, T., Chen, L., & Du, H. (2021). Virulence Factors in Hypervirulent Klebsiella pneumoniae. *Frontiers in Microbiology*, *12*, 642484. https://doi.org/10.3389/fmicb.2021.642484